General Eigenvalue Equations for Optical Planar Waveguides with Arbitrarily Graded-Index Profiles

Min-Sub Chung and Chang-Min Kim

***Abstract*—Accurate eigenvalue equations for planar waveguides with arbitrarily graded-index profile are derived and expressed in closed forms. A combination of the modified Airy functions and the Wenzel–Kramers–Brillouin (WKB) solutions are employed as field solutions, which turn out to represent almost exact field profiles. The use of new trial solutions enables us to calculate phase shifts at turning points very precisely, allowing us almost exact eigenvalues. It is demonstrated that the results obtained by the proposed method are in excellent agreement with those by the finite element method, achieving significant improvement over the conventional WKB method.**

***Index Terms*—Eigenvalue/eigenfunction, graded-index profile, modified Airy functions, planar waveguides, Wenzel–Kramers–Brillouin (WKB) method.**

I. Introduction

GUIDED modes of optical waveguides can be analyzed either by numerical techniques such as the finite element method (FEM), or by purely mathematical treatments. Numerical techniques guarantee higher accuracy as long as larger memories are available. These methods are not, however, so successful in delivering physical insights throughout the analytical procedure. Mathematical treatments are attractive in this respect since each mathematical expression is accompanied by a corresponding physical meaning. Among mathematical treatments, the Wenzel–Kramers–Brillouin (WKB) method has been extensively used and is still popular with many scientists as the method is simple in its derivation and gives reasonably accurate results under the condition of slow index variations across waveguides [1]–[9].

In the WKB method, appropriate trial solutions are defined depending on regions separated by turning points. The field solutions are expressed by the asymptotic forms of the Airy functions when the field point is far away from the turning point. The asymptotic field expressions enable us to obtain its eigenvalue equation in concise integral forms by imposing the proper boundary conditions. Unfortunately, this method yields large errors for a fundamental mode and for other modes near their cutoffs, since the field solutions diverge at a turning point and the phase shift at a turning point in graded slopes is fixed to be a constant value of $\pi/4$. To improve these inherent errors of the conventional WKB approximation, the authors in [4] introduced the concept of virtual turning points and tried to express fields near index discontinuities elaborately, thereby reducing the errors in the conventional WKB method significantly. However, the introduction of virtual turning points in their method not only brought about the complexity in the derivation of eigenvalue equations, but also yielded the ambiguity in appreciating the field solutions.

More rigorous solutions by the modified airy functions (MAF's) were first proposed by Langer [5] and have recently been used by several researchers. Roy *et al.*employed the MAF to calculate tunneling coefficients [6]. Goyal *et al.* improved the accuracy of the MAF by readjusting the argument of the Airy functions, although trial solutions were not presented in cladding regions [7].

In this paper, we present a mathematical yet rigorous analytical procedure for planar waveguides with arbitrarily graded index profiles and derive the closed form of general eigenvalue equations. In our analysis, a new set of field solutions are employed, a combination of the modified Airy functions and the conventional WKB solutions. In the region of a core, the modified Airy functions are employed to describe wave form properly. In cladding regions, the conventional WKB solutions are used to ensure the field to decay in an exponential form. It turns out that the defined field solutions of the proposed method not only converge at turning points but also present very accurate field solutions, thus improving the precision of phase shifts at turning points. Analyzes by the conventional WKB method and the FEM are also performed to enable comparison. It is demonstrated through computer simulations that results obtained by the proposed method agree well with those by the FEM, showing significant improvement over the conventional WKB method.

II. Derivation of Eigenvalue Equations

One-dimensional (1-D) Helmholtz equation for planar waveguides with arbitrary index profile is

$$\frac{d^2}{dx^2}\,E(x) + \Gamma^2(x)E(x) = 0 \tag{1}$$

where

$$\Gamma^2(x) = k_0^2(n^2(x) - N^2). \tag{2}$$

In (2), N is the mode index. $n^2(x)$ denotes refractive index profile and typical figures are plotted in Fig. 1. In the figure, is arbitrarily positioned between two turning points.

Case A: $a < x_{t1}, x_{t2} < b$ as in Fig. 1

Manuscript received February 27, 1999; revised March 14, 2000. This work was supported by the 1998 University Research Program, Ministry of Information and Communication.

The authors are with the Department of Electronics Engineering, The University of Seoul, Seoul 130-743, Korea.

Publisher Item Identifier S 0733-8724(00)05078-7.

0733–8724/00$10.00 © 2000 IEEE

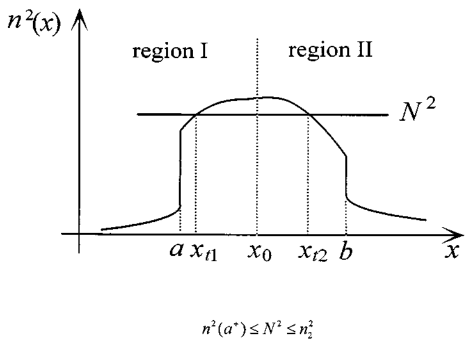

Fig. 1. Index profile $n^2(x)$ and a mode index N. Turning points $a < x_{t1}$, $x_{t2} < b$.

Field solutions for each region may be put as (3a)–(3c) and (4a)–(4c), as shown at the bottom of the page, where

$$\eta_i(x) = \left(\frac{3}{2}\,(-1)^i \int_{x_{ti}}^{x} P(x)\,dx\right)^{2/3}$$
$$P(x) = \sqrt{-\Gamma^2(x)}, \qquad i = 1, 2 \tag{5a}$$

$$\xi_i(x) = \left(\frac{3}{2}\,(-1)^{i-1} \int_{x_{ti}}^{x} Q(x)\,dx\right)^{2/3}$$
$$Q(x) = \sqrt{\Gamma^2(x)}, \qquad i = 1, 2. \tag{5b}$$

Field solutions $E_{\rm I}(x)$ and $E_{\rm II}(x)$ decay exponentially in regions $x \le a$, $x \ge b$. In regions $a \le x \le x_{t1}$ and $x_{t2} \le x \le b$, we use the modified Airy functions with positive argument to express a combination of purely decreasing and increasing properties, respectively. Field solutions in $x_{t1} < x < x_{t2}$ need to show oscillatory natures and, therefore, are expressed in terms of the modified Airy functions with negative argument. The modified Airy functions are most suitable for describing field behaviors in guided regions since the functions not only converge at turning points but also their asymptotes yield the same field expressions as in the WKB method. Asymptotic forms of the modified Airy functions are expressed as follows:

$$\frac{1}{\sqrt{(-1)^{i-1}\xi_i'(x)}}\,Ai(-\xi_i(x)) \Rightarrow \frac{1}{\sqrt{\pi Q(x)}}\,\sin\left((-1)^{i-1}\int_{x_{ti}}^{x} Q(x)\,dx + \frac{\pi}{4}\right) \tag{6a}$$

$$\frac{1}{\sqrt{(-1)^{i-1}\xi_i'(x)}}\,Bi(-\xi_i(x)) \Rightarrow \frac{1}{\sqrt{\pi Q(x)}}\,\cos\left((-1)^{i-1}\int_{x_{ti}}^{x} Q(x)\,dx + \frac{\pi}{4}\right). \tag{6b}$$

When a field point is far away from both turning points, (3c) and (4a) can be replaced by a linear combination of the sinusoidal functions in (6). By imposing the boundary condition that $E_{\rm I}(x)$ and $E_{\rm II}(x)$ and their derivatives should be continuous at $x = x_0$, we obtain the following:

i)

$$\begin{aligned} E_{\rm I}(x)|_{x=x_0^-} &= E_{\rm II}(x)|_{x=x_0^+} \\ &\Rightarrow c_2\,\sin\left(\int_{x_{t1}}^{x_0^-} Q(x)\,dx + \frac{\pi}{4}\right) \\ &\quad + c_3\,\cos\left(\int_{x_{t1}}^{x_0^-} Q(x)\,dx + \frac{\pi}{4}\right) \\ &= c_4\,\sin\left(\int_{x_0^+}^{x_{t2}} Q(x)\,dx + \frac{\pi}{4}\right) \\ &\quad + c_5\,\cos\left(\int_{x_0^+}^{x_{t2}} Q(x)\,dx + \frac{\pi}{4}\right) \end{aligned} \tag{7}$$

$$E_{\rm I}(x) = \begin{cases} \dfrac{c_1}{2\sqrt{\pi P(x)}}\,\exp\left(-\displaystyle\int_x^a P(x)\,dx\right) & x \le a \quad (3a) \\ \dfrac{c_2}{\sqrt{-\eta_1'(x)}}\,Ai(\eta_1(x)) + \dfrac{c_3}{\sqrt{-\eta_1'(x)}}\,Bi(\eta_1(x)) & a \le x \le x_{t1} \quad (3b) \\ \dfrac{c_2}{\sqrt{\xi_1'(x)}}\,Ai(-\xi_1(x)) + \dfrac{c_3}{\sqrt{\xi_1'(x)}}\,Bi(-\xi_1(x)) & x_{t1} \le x \le x_0 \quad (3c) \end{cases}$$

$$E_{\rm II}(x) = \begin{cases} \dfrac{c_4}{\sqrt{-\xi_2'(x)}}\,Ai(-\xi_2(x)) + \dfrac{c_5}{\sqrt{-\xi_2'(x)}}\,Bi(-\xi_2(x)) & x_0 \le x \le x_{t2} \quad (4a) \\ \dfrac{c_4}{\sqrt{\eta_2'(x)}}\,Ai(\eta_2(x)) + \dfrac{c_5}{\sqrt{\eta_2'(x)}}\,Bi(\eta_2(x)) & x_{t2} \le x \le b \quad (4b) \\ \dfrac{c_6}{2\sqrt{\pi P(x)}}\,\exp\left(-\displaystyle\int_b^x P(x)\,dx\right) & x \ge b \quad (4c) \end{cases}$$

ii)

$$\frac{d}{dx}\,E_{\rm I}(x)|_{x=x_0^-}=\frac{d}{dx}\,E_{\rm II}(x)|_{x=x_0^+}$$
$$\Rightarrow c_2\;\cos\left(\int_{x_{t1}}^{x_0^-}\,Q(x)\,dx+\frac{\pi}{4}\right)$$
$$-\,c_3\;\sin\left(\int_{x_{t1}}^{x_0^-}\,Q(x)\,dx+\frac{\pi}{4}\right)$$
$$=-\,c_4\;\cos\left(\int_{x_0^+}^{x_{t2}}\,Q(x)\,dx\;+\frac{\pi}{4}\right)$$
$$+\,c_5\;\sin\left(\int_{x_0^+}^{x_{t2}}\,Q(x)\,dx+\frac{\pi}{4}\right). \tag{8}$$

Dividing (7) by (8) and manipulating, we have

$$\tan\left(\int_{x_{t1}}^{x_0^-}\,Q(x)\,dx-\tan^{-1}\left(-\frac{c_3}{c_2}\right)\right)$$
$$=\tan\left(\int_{x_{t1}}^{x_0^-}\,Q(x)\,dx\right.$$
$$\left.-\left(\int_{x_{t1}}^{x_{t2}}\,Q(x)\,dx-\tan^{-1}\left(-\frac{c_5}{c_4}\right)-\frac{\pi}{2}\right)\right). \tag{9}$$

Further manipulation leads us to the eigenvalue equation of

$$\int_{x_{t1}}^{x_{t2}}\,Q(x)\,dx=m\pi+\left(\frac{\pi}{4}+\delta_1\right)+\left(\frac{\pi}{4}+\delta_2\right). \tag{10}$$

Phase shift term δ_1 and δ_2 at each turning point are calculated to be

$$\delta_1=\tan^{-1}\left(-\frac{c_3}{c_2}\right) \tag{11a}$$

$$\delta_2=\tan^{-1}\left(-\frac{c_5}{c_4}\right). \tag{11b}$$

Applying the continuity of $E_{\rm I}(x)$ and $E_{\rm I}'(x)$ at $x=a$, we can obtain the expression of δ_1 in a closed form. The continuity of $E_{\rm II}(x)$ and $E_{\rm II}'(x)$ at $x=b$ also leads us to the expression of δ_2.

i)

$$E_{\rm I}(x)|_{x=a^-}=E_{\rm I}(x)|_{x=a^+}$$
$$\Rightarrow\;\frac{c_1}{2\sqrt{\pi P(x)}}\;\exp\left(-\int_x^a\,P(x)\,dx\right)\Bigg|_{x=a^-}$$
$$=\frac{c_2}{\sqrt{-\eta_1'(x)}}\,Ai(\eta_1(x))+\frac{c_3}{\sqrt{-\eta_1'(x)}}\,Bi(\eta_1(x))|_{x=a^+} \tag{12}$$

ii)

$$\frac{d}{dx}\,E_{\rm I}(x)\Big|_{x=a^-}=\frac{d}{dx}\,E_{\rm I}(x)\Big|_{x=a^+}$$
$$\Rightarrow\frac{1}{2}\exp\left(-\int_x^a\,P(x)\,dx\right)$$
$$\cdot\left\{-\frac{1}{2}\,\frac{c_1P'(x)}{P(x)\sqrt{\pi P(x)}}+\frac{c_1P(x)}{\sqrt{\pi P(x)}}\right\}\Bigg|_{x=a^-}$$
$$=\frac{c_2}{\sqrt{-\eta_1'(x)}}\left\{-\frac{\eta''(x)}{2\eta_1'(x)}Ai(\eta_1(x))\right.$$
$$\left.+\eta_1'(x)Ai'(\eta_1(x))\right\}$$
$$+\frac{c_3}{\sqrt{-\eta_1'(x)}}\left\{-\frac{\eta_1''(x)}{2\eta_1'(x)}\,Bi(\eta_1(x))\right.$$
$$\left.+\eta_1'(x)Bi'(\eta_1(x))\right\}\Bigg|_{x=a^+}. \tag{13}$$

From (12) and (13), c_3/c_2 is deduced and δ_1 is accordingly expressed as a combination of Airy functions and their derivatives

$$\delta_1=\tan^{-1}\left\{\frac{-\eta_1'(a^+)Ai'(\eta_1(a^+))+P_aAi(\eta_1(a^+))}{-\eta_1'(a^+)Bi'(\eta_1(a^+))+P_aBi(\eta_1(a^+))}\right\} \tag{14}$$

where

$$P_a=P(a^-)-\frac{1}{2}\,\left\{\frac{P'(a^-)}{P(a^-)}-\frac{\eta_1''(a^+)}{\eta_1'(a^+)}\right\}. \tag{15}$$

Applying the boundary condition of $E_{\rm II}(x)$ at $x=b$, we deduce δ_2 as follows:

$$\delta_2=\tan^{-1}\left\{\frac{\eta_2'(b^-)Ai'(\eta_2(b^-))+P_bAi(\eta_2(b^-))}{\eta_2'(b^-)Bi'(\eta_2(b^-))+P_bBi(\eta_2(b^-))}\right\} \tag{16}$$

where

$$P_b=P(b^+)+\frac{1}{2}\,\left\{\frac{P'(b^+)}{P(b^+)}-\frac{\eta_2''(b^-)}{\eta_2'(b^-)}\right\}. \tag{17}$$

Since $\eta_1'(a^+)=-\eta_2'(b^-)$, and $P'(a^-)=-P'(b^+)$ for symmetric profile, δ_1 becomes equal to δ_2. δ_i of (14) and (16) are represented in terms of Airy functions and their derivatives, and the expression of δ_i may be expanded in terms of Bessel functions (Appendix A).

In case of $c_3=c_5=0$ in (3) and (4), it follows that $\delta_1=\delta_2=0$. In such a case, the eigenfunctions and corresponding eigenvalue equations of (10) become the results of the conventional WKB method. While the phase shift at every turning point in the WKB method becomes the fixed value of $\pi/4$ regardless of the relative position of a mode index, the phase shift by the proposed method becomes a variable value of $(\pi/4+\delta_i)$ and this δ_i reflects the influence of the relative position of an obtained mode index.

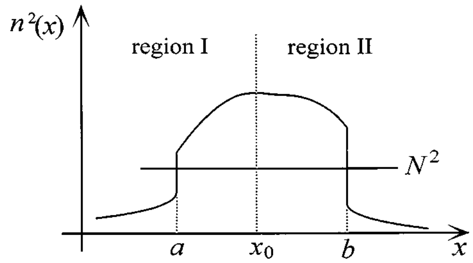

$n^2(a^-) \leq N^2 \leq n^2(a^+)$

Fig. 2. Index profile $n^2(x)$ and a mode index N turning points $x = a, x = b$.

Case B: $x = a$, $x = b$ as in Fig. 2

This is the case where both turning points are on index discontinuities. In this case, field solutions of $E_{\rm I}(x)$ and $E_{\rm II}(x)$ are decreasing exponentially outward in the regions of $x \leq a$ and $x \geq b$, and show oscillatory behavior in the region of $a \leq x \leq b$. To preserve consistency with the contents of Case A, trial solutions in this case are expressed as a functions of asymptotes of the Airy functions. Field functions are then represented by (18a) and (18b) and (19a) and (19b) shown at the bottom of the page.

Imposing the boundary conditions that $E_{\rm I}(x)$ and $E_{\rm II}(x)$ and their derivatives are continuous at $x = x_0$, we come to have an eigenvalue equation of

$$\int_a^b Q(x)\,dx = m\pi + \left(\frac{\pi}{4} + \delta_1\right) + \left(\frac{\pi}{4} + \delta_2\right). \tag{20}$$

Definition of δ_1 and δ_2 are same as in (11). c_3/c_2 and c_5/c_4 are calculated from the boundary conditions on $E_{\rm I}(x)$ at $x = a$ and $E_{\rm II}(x)$ at $x = b$, respectively. Following the same procedure as Case A, we have the expressions of δ_1 and δ_2 as

$$\delta_1 = -\frac{\pi}{4} + \tan^{-1}\left\{\frac{P_a}{Q(a^+)}\right\} \tag{21}$$

where

$$P_a = P(a^-) - \frac{1}{2}\left\{\frac{P'(a^-)}{P(a^-)} - \frac{Q'(a^+)}{Q(a^-)}\right\} \tag{22}$$

$$\delta_2 = -\frac{\pi}{4} + \tan^{-1}\left\{\frac{P_b}{Q(b^-)}\right\} \tag{23}$$

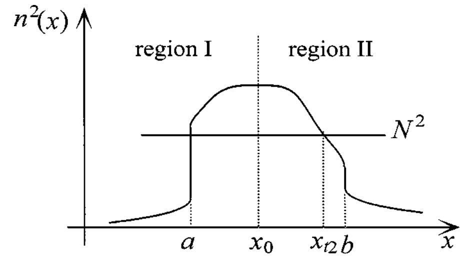

$n^2(b^-) \leq N^2 \leq n^2(a^+)$

(a)

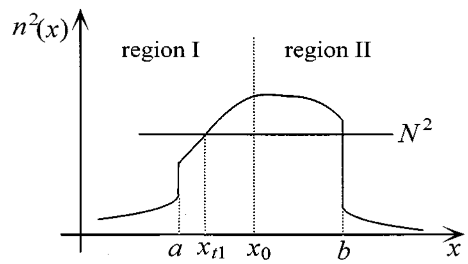

$n^2(a^+) \leq N^2 \leq n^2(b^-)$

(b)

Fig. 3. Index profile $n^2(x)$ and a mode index N (a) $x_{t1} = a, a < x_{t2} < b$, (b) $a < x_{t1} < b, x_{t2} = b$.

where

$$P_b = P(b^+) + \frac{1}{2}\left\{\frac{P'(b^+)}{P(b^+)} - \frac{Q'(b^-)}{Q(b^-)}\right\} \tag{24}$$

In case of a step index profile, P_a and P_b of (22) and (24) become $P(a^-)$ and $P(b^+)$, respectively. Hence, when inserting these results into (21) and (23), (20) yields the same eigenvalue equation as is obtained by directly solving the Helmholtz equation of (1).

Case C: $x_{t1} = a$ and $a < x_{t2} < b$, or $a < x_{t1} < b$ and $x_{t2} = b$ as in Fig. 3.

Typical cases are plotted in Fig. 3, where one of two turning points is at a discontinuity in the index profile. is positioned arbitrarily between two turning points.

$$E_{\rm I}(x) = \begin{cases} \dfrac{c_1}{2\sqrt{\pi P(x)}}\,\exp\left(-\displaystyle\int_x^a P(x)\,dx\right) & x \leq a \quad (18a) \\ \dfrac{c_2}{\sqrt{\pi Q(x)}}\,\sin\left(\displaystyle\int_a^x Q(x)\,dx + \frac{\pi}{4}\right) + \dfrac{c_3}{\sqrt{\pi Q(x)}}\,\cos\left(\displaystyle\int_a^x Q(x)\,dx + \frac{\pi}{4}\right) & a \leq x \leq x_0 \quad (18b) \end{cases}$$

$$E_{\rm II}(x) = \begin{cases} \dfrac{c_4}{\sqrt{\pi Q(x)}}\,\sin\left(\displaystyle\int_x^b Q(x)\,dx + \frac{\pi}{4}\right) + \dfrac{c_5}{\sqrt{\pi Q(x)}}\,\cos\left(\displaystyle\int_x^b Q(x)\,dx + \frac{\pi}{4}\right) & x_0 \leq x \leq b \quad (19a) \\ \dfrac{c_6}{2\sqrt{\pi P(x)}}\,\exp\left(-\displaystyle\int_b^x P(x)\,dx\right) & b \leq x \quad (19b) \end{cases}$$

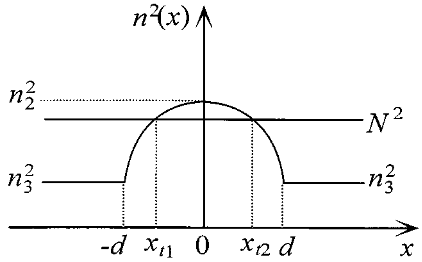

Fig. 4. A symmetrically parabolic index profile.

In the case of Fig. 3(a), $x_{t1} = a$ and $a < x_{t2} < b$. Field solutions of the region I and the region II are the same as (18) and (4), respectively. From the condition of field continuity at $x = x_0$ and boundary conditions at $x = a$ and $x = b$, an eigenvalue equation is derived as follows:

$$\int_{a}^{x_{t2}} Q(x)\,dx = m\pi + \left(\frac{\pi}{4} + \delta_1\right) + \left(\frac{\pi}{4} + \delta_2\right) \tag{25}$$

where δ_1 and δ_2 in (25) are the same with (21) and (16), respectively.

In the case of Fig. 3(b), $a < x_{t1} < b$ and $x_{t2} = b$. $E_{\mathrm{I}}(x)$ and $E_{\mathrm{II}}(x)$ are the same with (3) and (19). From the boundary condition at $x = x_0$, the eigenvalue equation is obtained as follows:

$$\int_{x_{t1}}^{b} Q(x)\,dx = m\pi + \left(\frac{\pi}{4} + \delta_1\right) + \left(\frac{\pi}{4} + \delta_2\right) \tag{26}$$

where δ_1 and δ_2 are deduced to be the same expression as (14) and (23).

III. Numerical Simulations

In order to evaluate the accuracy of eigenvalue equations and their corresponding eigenfunctions obtained in Section II, we take two types of waveguide index profiles as examples, a symmetrically parabolic and a truncated parabolic index profile.

Case A: Symmetrically Parabolic Index Profile:: Index profile for Fig. 4 may be given by

$$n^2(x) = \begin{cases} n_3^2, & x \le -d \\ n_3^2 + (n_2^2 - n_3^2)\left(1 - \left(\dfrac{x}{d}\right)^2\right), & -d \le x \le d \\ n_3^2, & x \ge d \end{cases} \tag{27}$$

For this index distribution, the field solutions follow the expressions of (3) and (4), and the eigenvalue equation corresponds to (10). For the sake of convenience in computation, the eigenvalue equation is rewritten as a function of the normalized frequency v and the normalized propagation constant b shown in (28) at the bottom of the page where

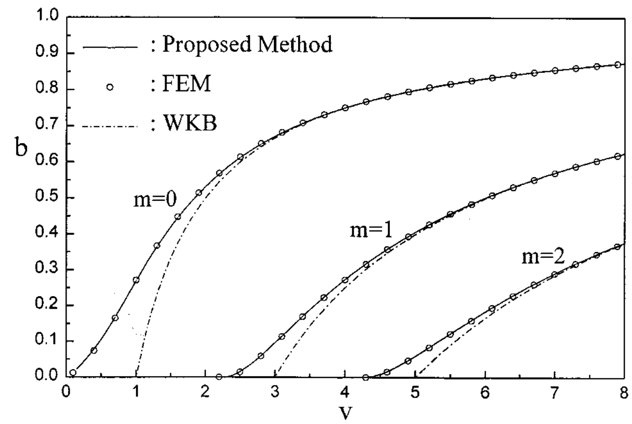

Fig. 5. v–b curves for waveguides with symmetrically parabolic index profile.

$$\varphi(d^-) = \int_{x_{t2}}^{d^-} P(x)\,dx \tag{29}$$

$$\rho_2 = 1 - \frac{1}{2}\,\frac{1}{\mathrm{v}\mathrm{b}\sqrt{\mathrm{b}}} + \frac{1}{6\varphi(d^-)} \tag{30}$$

v and b are conventionally defined by

$$\mathrm{v} = k_0 d\sqrt{n_2^2 - n_3^2} \tag{31}$$

$$\mathrm{b} = \frac{N^2 - n_3^2}{n_2^2 - n_3^2}. \tag{32}$$

Physical quantities of δ_1 and δ_2 are equal although they look different in mathematical expression since the index profile is symmetric. δ_i is expressed to be the arctangent term in (28) independent of index profile shape.

v–b curves calculated from (28) for waveguides with symmetrically parabolic index profile are illustrated in Fig. 5. Accurate results obtained by the FEM are plotted for reference and results by the conventional WKB method are drawn as well for comparison's purpose. It is shown that results obtained by the proposed method are in excellent agreement with those by the FEM.

Field profiles for the fundamental and first-order modes are shown in Fig. 6(a) and (b), respectively. It is observed that field profiles obtained by the proposed method not only converge at the turning points but also coincide with those by the FEM, while the field forms calculated by the conventional WKB method diverge at the turning point.

$$\mathrm{v}(1-\mathrm{b}) = (2m+1) + \frac{4}{\pi} \cdot \tan^{-1}\left\{ \frac{1}{\sqrt{3}}\; \frac{-(\rho_2\varphi(d^-) + \frac{2}{3})I_{1/3}(\varphi(d^-)) + (\varphi(d^-) + \frac{4}{3}\,\rho_2)I_{2/3}(\varphi(d^-)) - \varphi(d^-)I_{4/3}(\varphi(d^-)) + \rho_2\varphi(d^-)I_{5/3}(\varphi(d^-))}{(\rho_2\varphi(d^-) + \frac{2}{3})I_{1/3}(\varphi(d^-)) + (\varphi(d^-) + \frac{4}{3}\,\rho_2)I_{2/3}(\varphi(d^-)) + \varphi(d^-)I_{4/3}(\varphi(d^-)) + \rho_2\varphi(d^-)I_{5/3}(\varphi(d^-))} \right\} \tag{28}$$

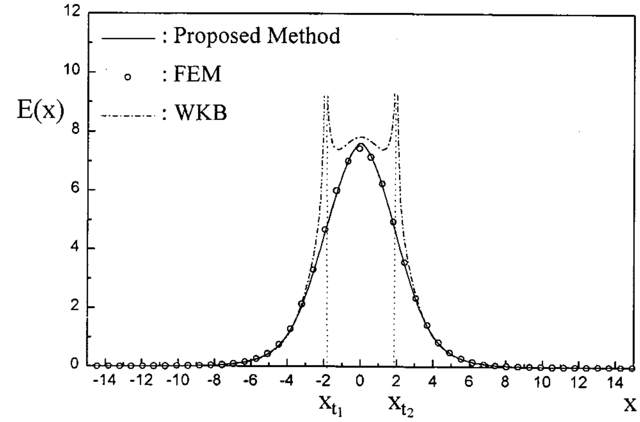

(a) $m=0$

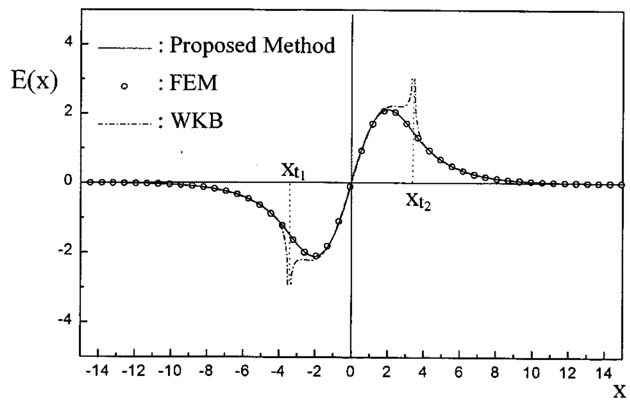

(b) $m=1$

Fig. 6. Field profiles of waveguides with symmetrically parabolic index profile at v $= 4.0$.

Case B: Truncated Parabolic Index Profile: Index profile of Fig. 7 may be expressed as

$$n^2(x) = \begin{cases} n_1^2, & x \le 0 \\ n_3^2 + (n_2^2 - n_3^2)\left(1 - \left(\dfrac{x}{d}\right)^2\right), & 0 \le x \le d \\ n_3^2, & x \ge d. \end{cases} \tag{33}$$

Field trial solutions are given as in (18) and (4) in this case, and the eigenvalue equation is same as (25). Under the assumption of $N^2 - n_3^2 \gg N^2 - n_1^2$, as is mostly the case, (25) is expressed in terms of v and b as below.

$$\mathrm{v}(1-\mathrm{b}) = (4m+3) + [\text{last term of (28) }] \tag{34}$$

v–b curves calculated from (34) for the waveguides with truncated parabolic index profile are presented in Fig. 8. The dispersion curves obtained by the proposed method are exactly coincident with those by the FEM, while the conventional WKB method still fails to give a reasonable accuracy near the cutoff regions.

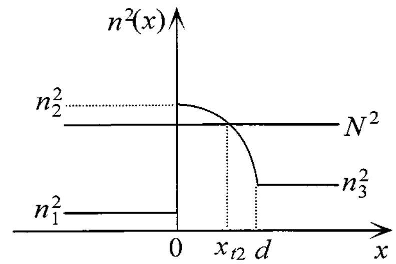

Fig. 7. A truncated parabolic index profile.

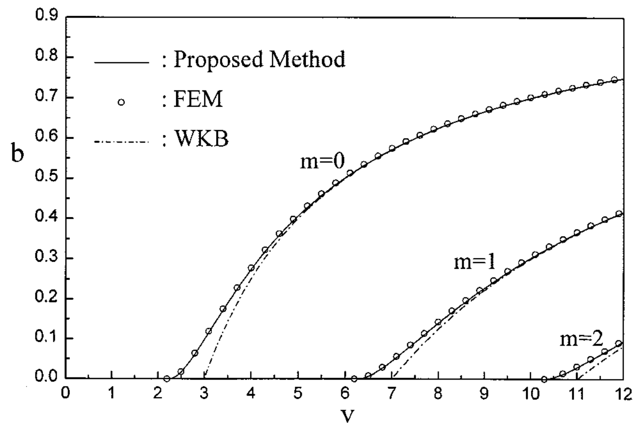

Fig. 8. v–b curves for waveguides with truncated parabolic index profile.

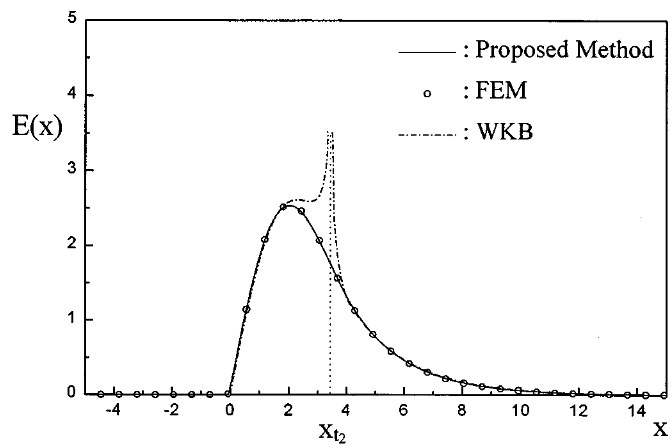

Fig. 9. Field profiles of waveguides with truncated parabolic index profile at v $= 4.0$.

Field profiles are plotted for v $= 4.0$ in Fig. 9 to confirm again the precision of the proposed method. As shown in the figure, the results exactly overlap with that obtained by the FEM, while the field profiles by the WKB method diverge at the turning point.

IV. Discussions

A mathematically rigorous and physically intuitive analysis for optical planar waveguides with arbitrary index profiles is presented. A combination of the modified Airy functions and the WKB solutions are employed as eigenfunctions to ensure correct phase shift at turning points, which consequently leads us to precise eigenvalue equations. Through the numerical analysis, it is demonstrated that v–b curves obtained by the proposed method excellently agree with those by the finite element method, while the results calculated by the conventional WKB method yields large errors, especially for the fundamental mode and for other modes near their cutoff. It also turns out that field solutions obtained by our method are very accurate when compared with the exact field profiles by the finite element method.

APPENDIX A

δ_1 REPRESENTATION IN TERMS OF BESSEL FUNCTIONS

Recursive equations of Bessel functions are

$$2I'_\nu(z) = I_{\nu-1}(z) + I_{\nu+1}(z) \tag{A1}$$

$$\frac{2\nu}{z}\, I_\nu(z) = I_{\nu-1}(z) - I_{\nu+1}(z). \tag{A2}$$

Using the (A1) and (A2), $Ai(y)$, $Ai'(y)$, $Bi(y)$, and $Bi'(y)$ are expressed in terms of Bessel functions as follows:

$$\begin{aligned} Ai(y) &= \frac{\sqrt{y}}{3}\,(I_{-1/3}(z) - I_{1/3}(z)) \\ &= \frac{\sqrt{y}}{3z}\,\left\{-zI_{1/3}(z) + \frac{4}{3}\,I_{2/3}(z) + zI_{5/3}(z)\right\} \end{aligned} \tag{A3}$$

$$\begin{aligned} Ai'(y) &= \frac{1}{6\sqrt{y}}\,(I_{-1/3}(z) - I_{1/3}(z)) \\ &\quad + \frac{y}{3}\,(I'_{-1/3}(z) - I'_{1/3}(z)) \\ &= \frac{y}{3z}\,\left\{-\frac{2}{3}\,I_{1/3}(z) + zI_{2/3}(z) - zI_{4/3}(z)\right\} \end{aligned} \tag{A4}$$

$$\begin{aligned} Bi(y) &= \frac{\sqrt{y}}{\sqrt{3}}\,(I_{-1/3}(z) + I_{1/3}(z)) \\ &= \frac{\sqrt{y}}{\sqrt{3}z}\,\left\{zI_{1/3}(z) + \frac{3}{4}\,I_{2/3}(z) + zI_{5/3}(z)\right\} \end{aligned} \tag{A5}$$

$$\begin{aligned} Bi'(y) &= \frac{\sqrt{3}}{6\sqrt{y}}\,(I_{-1/3}(z) + I_{1/3}(z)) \\ &\quad + \frac{y}{3}\,(I'_{-1/3}(z) + I'_{1/3}(z)) \\ &= \frac{y}{\sqrt{3}z}\,\left\{\frac{2}{3}\,I_{1/3}(z) + zI_{2/3}(z) + zI_{4/3}(z)\right\} \end{aligned} \tag{A6}$$

where

$$z = \tfrac{2}{3}\,y^{3/2} \tag{A7}$$

With the aid of (A1)–(A6), we change the denominator and numerator in to more easily calculable forms.

i) Terms in the numerator

$$\begin{aligned} &\eta'_2(b^-)Ai'(\eta_2(b^-)) \\ &\quad = \frac{\sqrt{\eta_2(b^-)}}{3\varphi(b^-)}\,P(b^-)\left\{-\frac{2}{3}\,I_{1/3}(\varphi(b^-)) \right. \\ &\qquad \left. + \varphi(b^-)I_{2/3}(\varphi(b^-)) - \varphi(b^-)I_{4/3}(\varphi(b^-))\right\} \end{aligned} \tag{A8}$$

$$\begin{aligned} &P_bAi(\eta_2(b^-)) \\ &\quad = \frac{\sqrt{\eta_2(b^-)}}{3\varphi(b^-)}\,P_b\left\{-\varphi(b^-)I_{1/3}(\varphi(b^-)) \right. \\ &\qquad \left. + \frac{4}{3}\,I_{2/3}(\varphi(b^-)) + \varphi(b^-)I_{5/3}(\varphi(b^-))\right\} \end{aligned} \tag{A9}$$

ii) Terms in the denominator

$$\begin{aligned} &\eta'_2(b^-)Bi'(\eta_2(b^-)) \\ &\quad = \frac{\sqrt{\eta_2(b^-)}}{\sqrt{3}\varphi(b^-)}\,P(b^-)\left\{-\frac{2}{3}\,I_{1/3}(\varphi(b^-)) \right. \\ &\qquad \left. + \varphi(b^-)I_{2/3}(\varphi(b^-)) + \varphi(b^-)I_{4/3}(\varphi(b^-))\right\} \end{aligned} \tag{A10}$$

$$\begin{aligned} &P_bBi(\eta_2(b^-)) \\ &\quad = \frac{\sqrt{\eta_2(b^-)}}{\sqrt{3}\varphi(b^-)}\,P_b\left\{\varphi(b^-)I_{1/3}(\varphi(b^-)) \right. \\ &\qquad \left. + \frac{4}{3}\,I_{2/3}(\varphi(b^-)) + \varphi(b^-)I_{5/3}(\varphi(b^-))\right\} \end{aligned} \tag{A11}$$

Substituting (A8)–(A11) into δ_2 of (16) and manipulating, we have (A12) shown at the bottom of the page where

$$\rho_2 = \frac{P_b}{P(b^-)} = \frac{1}{P(b^-)}\left[P(b^+) + \frac{1}{2}\left\{\frac{P'(b^+)}{P(b^+)} - \frac{\eta''_2(b^-)}{\eta'_2(b^-)}\right\}\right] \tag{A13}$$

$$\varphi(b^-) = \int_{x_{t2}}^{b^-} P(x)\,dx \tag{A14}$$

ρ_2 can again be represented as a function of only $P(b)$

$$\rho_2 = \frac{P(b^+)}{P(b^-)} + \frac{P'(b^+)}{2P(b^+)P(b^-)} - \frac{P'(b^-)}{2P^2(b^-)} + \frac{1}{6\varphi(b^-)}. \tag{A15}$$

δ_1 can also be obtained by following the same procedure as above. δ_1 is then represented by the same form as (A12), except that the variables ρ_2 and $\varphi(b^-)$ are replaced by ρ_1 and $\varphi(a^+)$, respectively.

$$\rho_1 = \frac{P_a}{P(a^+)} = \frac{P(a^-)}{P(a^+)} - \frac{P'(a^-)}{2P(a^-)P(a^+)} + \frac{P'(a^+)}{2P(a^+)} + \frac{1}{6\varphi(a^+)} \tag{A16}$$

$$\delta_2 = \tan^{-1}\left\{\frac{1}{\sqrt{3}}\;\frac{-(\rho_2\varphi(b^-) + \frac{2}{3})I_{1/3}(\varphi(b^-)) + (\varphi(b^-) + \frac{4}{3}\,\rho_2)I_{2/3}(\varphi(b^-)) - \varphi(b^-)I_{4/3}(\varphi(b^-)) + \rho_2\varphi(b^-)I_{5/3}(\varphi(b^-))}{(\rho_2\varphi(b^-) + \frac{2}{3})I_{1/3}(\varphi(b^-)) + (\varphi(b^-) + \frac{4}{3}\,\rho_2)I_{2/3}(\varphi(b^-)) + \varphi(b^-)I_{4/3}(\varphi(b^-)) + \rho_2\varphi(b^-)I_{5/3}(\varphi(b^-))}\right\} \tag{A12}$$

and

$$\varphi(a^+) = \int_{a^+}^{x_{t2}} P(x)\,dx. \tag{A17}$$

The fact that, for symmetric index profile, $P'(b^+) = -P'(a^-)$ and $P'(b^-) = -P'(a^+)$ leads to $\rho_1 = \rho_2$.

REFERENCES

[1] R. Srivastava, C. K. Kao, and R. V. Ramaswamy, "WKB analysis of planar surface waveguides with truncated index profiles," *J. Lightwave Technol.*, vol. LT-5, pp. 1605–1609, Nov. 1987.

[2] C. M. Kim and R. V. Ramaswamy, "WKB analysis of asymmetric directional couplers and its application to optical switches," *J. Lightwave Technol.*, vol. 6, pp. 1109–1118, June 1988.

[3] J. Wang and L. Qiao, "A refined WKB method for symmetric planar waveguides with truncated-index profiles and graded-index profiles," *IEEE J. Quantum Electron.*, vol. 27, pp. 878–883, Apr. 1991.

[4] F. Xiang and G. L. Yip, "A modified WKB method for the improved phase shift at a turning point," *J. Lightwave Technol.*, vol. 12, pp. 443–452, Mar. 1994.

[5] R. E. Langer, "On the asymptotic solutions of ordinary differential equations, with an application to the Bessel functions of large order," *Trans. Amer. Math. Soc.*, vol. 33, no. 99, pp. 23–64, 1931.

[6] S. Roy, A. K. Ghatak, I. C. Goyal, and R. L. Gallawa, "Modified Airy function method for the analysis of tunneling problems in optical waveguides and quantum-well structures," *IEEE J. Quantum Electron.*, vol. 29, pp. 340–345, Feb. 1993.

[7] I. C. Goyal, R. Jindal, and A. K. Ghatak, "Planar optical waveguides with arbitrary index profile: An accurate method of analysis," *J. Lightwave Technol.*, vol. 15, pp. 2179–2182, Nov. 1997.

[8] C. M. Kim and M. S. Chung, "Eigenvalue equations of N-parallel graded-index waveguides: WKB analysis," *IEEE J. Quantum Electron.*, vol. 33, pp. 1608–1613, Sept. 1997.

[9] M. S. Chung and C. M. Kim, "Analysis of optical fibers with graded-index profile by a combination of modified Airy functions and WKB solutions," *J. Lightwave Technol.*, vol. 17, pp. 2534–2541, Dec. 1999.

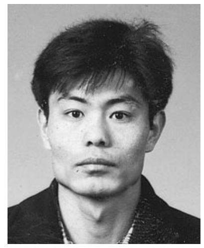

Min-Sub Chung was born in Haenam, Jeon-nam, Korea, in November 1970. He received the B.S. degree in electronics engineering from the University of Seoul, Korea, in 1995. He is currently working towards the M.S. degree in electronic engineering at the University of Seoul.

His current research interests include analytical treatment of Ti:LiNbO$_3$ optical waveguides, couplers, and switches.

Chang-Min Kim was born in Seoul, Korea, in April 1950. He received the B.S. and M.S. degrees in electronics engineering from the Seoul National University, Seoul, in 1975 and 1982, respectively, and the Ph.D. degree in electrical engineering from the University of Florida, Gainesville, in 1989.

He joined the faculty of the Department of Electronics Engineering at the University of Seoul in 1983 and is now a Professor. His research interests include analytical treatment and fabrication of Ti:LiNbO$_3$ optical waveguides, couplers, and high-speed optical switches/modulators.